Quantum Chaos and Realistic Quantum Computations

Dima Shepelyansky
CNRS Toulouse, FR (www.quantware.ups-tlse.fr)

Objective

- Effects of realistic imperfections on quantum computer operability and accuracy
- Decoherence and quantum chaos induced by inter-qubit couplings
- New efficient algorithms for simulation of quantum and classical physical systems
- Numerical codes with up to 30 qubits
- Development and test of error-correcting codes for quantum chaos and noisy gates

Objective Approach

- Analytical methods developed for many-body systems (nuclei, atoms, quantum dots)
- Random matrix theory and quantum chaos
- Large-scale numerical simulations of many qubits on modern supercomputers
- Stability of algorithms to quantum errors

Status

- RMT for quantum computations, universal law for fidelity decay induced by imperfections
- New quantum algorithms and imperfection effects for tent map, Grover algorithm; numerics with 7-28 qubits
- Pauli random error correction method

Quantware group at Toulouse

Laboratoire de Physique Théorique
UMR 5152 du CNRS, Université Paul Sabatier
Toulouse, France www.quantware.ups-tlse.fr

D.Braun, R.Fleckinger, K.Frahm (professors Univ. P.Sabatier)

B. Georgeot (researcher CNRS)

D.L.Shepelyansky (researcher CNRS, PI)

Jae-Weon Lee (EC EDIQIP post-doc => KIAS, Seoul)

J.Lages (EC EDIQIP post-doc), O.Giraud (post-doc => researcher CNRS)

A.Pomeransky (PhD => INP, Russia), B.Lévi (PhD => MIT)

A.D.Chepelianskii (undergraduate ENS, Ulm)

Collaboration: O.V.Zhirov (INP, Novosibirsk)

SUPPORT: EU IST-FET project EDIQIP

Quantum Hardware Melting Induced by Quantum Chaos

The quantum computer hardware is modeled as a (one)two-dimensional lattice of qubits (spin halves) with static fluctuations/imperfections in the individual qubit energies and residual short-range inter-qubit couplings. The model is described by the many-body Hamiltonian (B.Georgeot, D.S. PRE (2000)):

$$H_{\mathsf{S}} = \sum_i (\Delta_0 + \delta_i)\sigma_i^z + \sum_{i<j} J_{ij}\sigma_i^x\sigma_j^x,$$

where the σ_i are the Pauli matrices for the qubit i, and Δ_0 is the average level spacing for one qubit. The second sum runs over nearest-neighbor qubit pairs, and δ_i, J_{ij} are randomly and uniformly distributed in the intervals $[-\delta/2, \delta/2]$ and $[-J, J]$, respectively. Quantum chaos border for quantum hardware:

$$J > J_c \approx \Delta_c \approx 3\delta/n_q \gg \Delta_n \sim \delta 2^{-n_q}$$

Emergency rate of quantum chaos: $\Gamma \sim J^2/\Delta_c$.

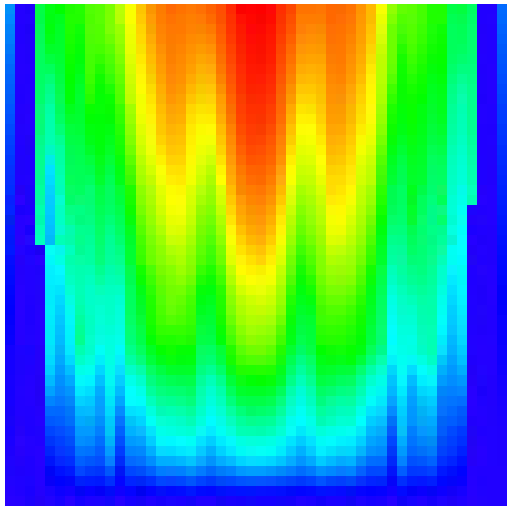

Quantum computer melting induced by inter-qubit couplings. Color represents the level of quantum eigenstate entropy S_q (red for maximum $S_q \approx 11$, blue for minimum $S_q = 0$). Horizontal axis is the energy of the computer eigenstates counted from the ground state to the maximal energy ($\approx 2n_q\Delta_0$). Vertical axis gives the value of J/Δ_0 (from 0 to 0.5). Here $n_q = 12$, $J_c/\Delta_0 = 0.273$, and one random realization of couplings is chosen.

What are effects of quantum many-body chaos
on the accuracy of quantum computations?
Static imperfections vs. random errors
in quantum gates of a quantum algorithm.

Elementary quantum gates

PHYSICAL REVIEW A VOLUME 54, NUMBER 1 JULY 1996

Quantum networks for elementary arithmetic operations

Vlatko Vedral,* Adriano Barenco, and Artur Ekert
Clarendon Laboratory, Department of Physics, University of Oxford, Oxford OX1 3PU, United Kingdom
(Received 3 November 1995)

Quantum computers require quantum arithmetic. We provide an explicit construction of quantum networks effecting basic arithmetic operations: from addition to modular exponentiation. Quantum modular exponentiation seems to be the most difficult (time and space consuming) part of Shor's quantum factorizing algorithm. We show that the auxiliary memory required to perform this operation in a reversible way grows linearly with the size of the number to be factorized. [S1050-2947(96)05707-1]

PACS number(s): 03.65.Ca, 07.05.Bx, 89.80.+h

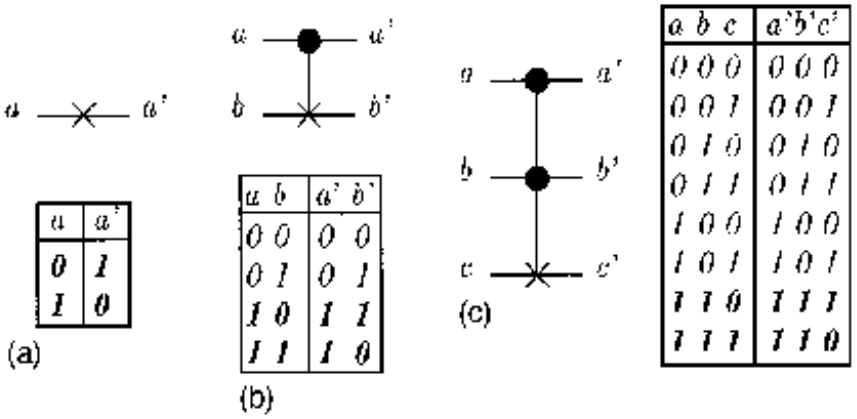

FIG. 1. Truth tables and graphical representations of the elementary quantum gates used for the construction of more complicated quantum networks. The control qubits are graphically represented by a dot, the target qubits by a cross. (a) NOT operation. (b) control-NOT. This gate can be seen as a "copy operation" in the sense that a target qubit (b) initially in the state 0 will be after the action of the gate in the same state as the control qubit. (c) Toffoli gate. This gate can also be seen as a control-control-NOT: the target bit (c) undergoes a NOT operation only when the two controls (a and b) are in state 1.

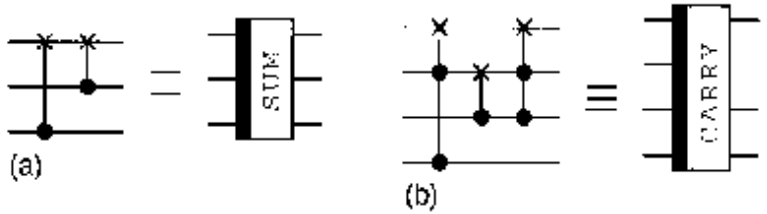

FIG. 3. Basic carry and sum operations for the plain addition network. (a) the carry operation (note that the carry operation perturbs the state of the qubit b). (b) the sum operation.

Fidelity decay due to errors

Accuracy measure of quantum computation is fidelity: $f(t) = |<\psi(t)|\psi_\varepsilon(t)>|^2$.

Quantum algorithm: $|\psi(t)> = U^t\,|\psi(0)>$, $U = \underbrace{U_{N_g} \cdot \ldots \cdot U_1}_{\text{elementary gates}}$.

Errors: $U_j \;\rightarrow\; U_j\, e^{i\delta H}$, $\delta H \sim \varepsilon$.

(i) Decoherence due to residual couplings of quantum computer to external bath:
δH random and different at each j and t,
e.g.: random phase fluctuations: $\delta\phi \in [-\varepsilon, \varepsilon]$ in phase-shift gates.

(ii) Static imperfections in the quantum computer itself:
δH (random but) constant at each j and t,
e.g.: $\delta H = \sum_{j=0}^{n_q-1} \delta_j\, \sigma_j^{(z)} + 2 \sum_{j=0}^{n_q-2} J_j\, \sigma_j^{(x)}\, \sigma_{j+1}^{(x)}$, $J_j, \delta_j \in [-\varepsilon, \varepsilon]$.

(iii) Non-unitary errors in quantum computation:
$e^{i\delta H}$ is non-unitary ($\delta H \neq \delta H^\dagger$, density matrix and quantum trajectories approach,
J.W.Lee, DS PRE **71**, 056202 (2005))

Example: model of quantum tent map

$$H(t) = \frac{T\,p^2}{2} + V(\theta) \sum_{n=-\infty}^{\infty} \delta(t-n)$$

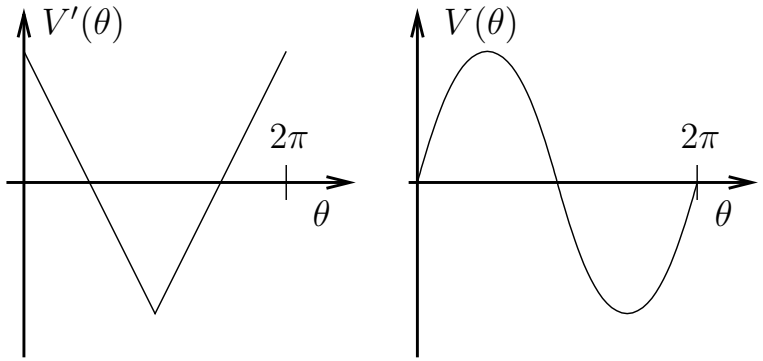

Classical map :

$$p_{n+1} = p_n - V'(\theta_n)$$
$$\theta_{n+1} = \theta_n + T\,p_{n+1}$$

Quantum map : $p = -i\partial/\partial\theta$

$$|\psi(t+1)> = U\,|\psi(t)>$$
$$U = e^{-iTp^2/2}\,e^{-iV(\theta)}$$

$$V(\theta) = \begin{cases} -\frac{k}{2}\theta(\theta-\pi) \\ \frac{k}{2}(\theta-\pi)(\theta-2\pi) \end{cases}, \quad V'(\theta) = \begin{cases} k(\frac{\pi}{2}-\theta) & \text{if} \quad 0 \le \theta \le \pi \\ k(-\frac{3\pi}{2}+\theta) & \text{if} \quad \pi \le \theta \le 2\pi \end{cases}$$

Quantum algorithm for tent (and saw-tooth) map

Quantum register identification: $|p> \equiv |\alpha_0>_0 \, |\alpha_1>_1 \, \ldots \, |\alpha_{n_q-1}>_{n_q-1}$.

$$p = \sum_{j=0}^{n_q-1} \alpha_j \, 2^j \;\in\; \{0, \ldots, N-1\}$$

$N = 2^{n_q}$ = dimension of Hilbert space; n_q = number of qubits; $\alpha_j \;\in\; \{0, 1\}$.

Quantum Fourier transform: $p \leftrightarrow \theta$ and $e^{-iTp^2/2} \, |p> = \prod_{j<k} \underbrace{e^{i(\cdots)\alpha_j\alpha_k}}_{B^{(2)}_{jk}(\cdots)} \prod_j \underbrace{e^{i(\cdots)\alpha_j}}_{B^{(1)}_j(\cdots)} \, |p>$.

with simple and controlled phase-shift:

$$B^{(1)}_j(\phi) = \begin{pmatrix} 1 & 0 \\ 0 & e^{i\phi} \end{pmatrix} \quad , \quad B^{(2)}_{jk}(\phi) = \begin{pmatrix} 1 & 0 & 0 & 0 \\ 0 & 1 & 0 & 0 \\ 0 & 0 & 1 & 0 \\ 0 & 0 & 0 & e^{i\phi} \end{pmatrix} .$$

Double controlled phase-shift: $B^{(3)}_{jkl}(\phi) = B^{(2)}_{jl}\left(\frac{\phi}{2}\right) \, B^{(2)}_{jk}\left(\frac{\phi}{2}\right) \, C^{(N)}_{kl} \, B^{(2)}_{jk}\left(-\frac{\phi}{2}\right) \, C^{(N)}_{kl}$.

Number of elementary gates: $n_g \approx 9\, n_q^2/2$

Husimi function

$t = 5$ 16 qubits $t = 15$

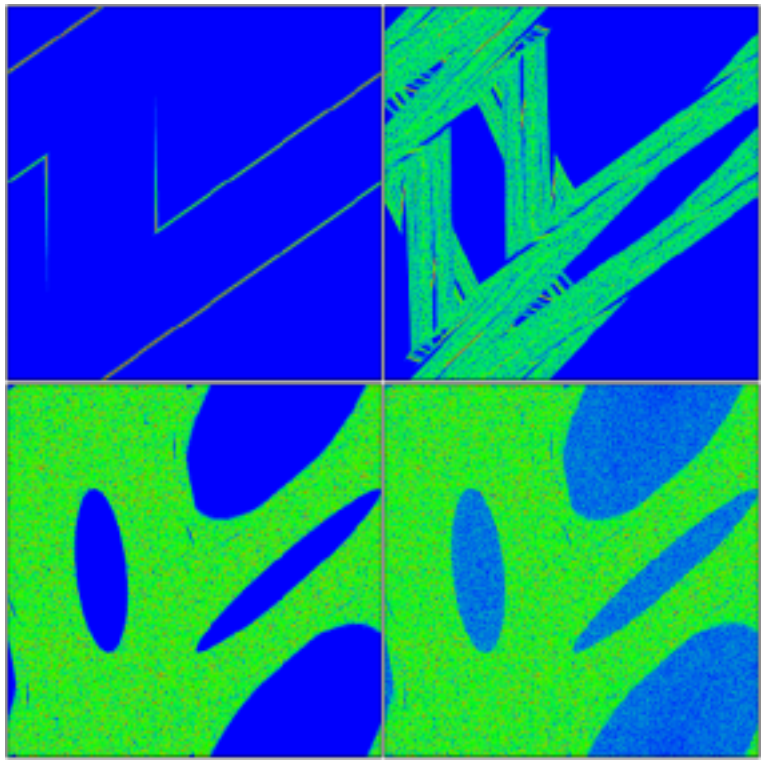

$t = 5625, \varepsilon = 0$ $\varepsilon = 7 \cdot 10^{-7}$

$\hbar_{\rm eff} = T = 2\pi/N, \;\; N = 2^{nq}$

Poincaré section $(K = kT = 1.7)$

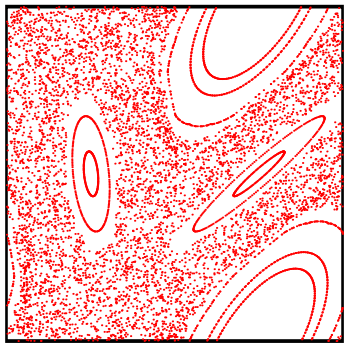

Fidelity decay with errors

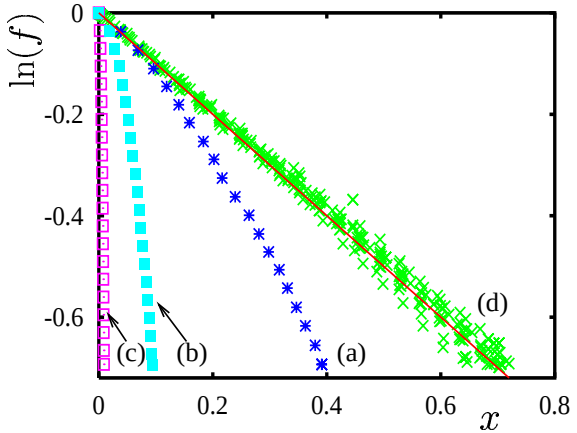

(static: $x = t/t_C$, (a), (b), (c),
random: $x = t/t_r$, (d))

Eigenstates of operating quantum computer: hypersensitivity to static imperfections

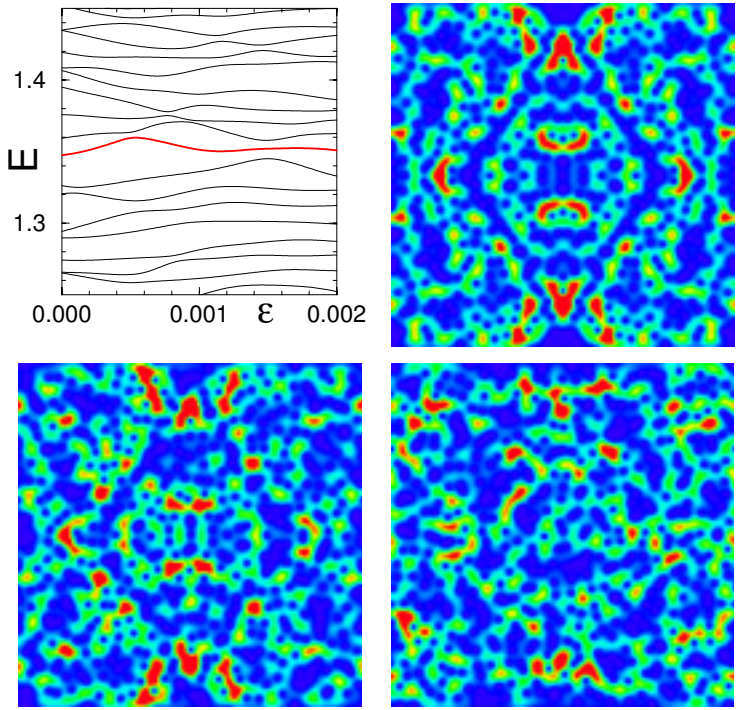

Variation of quasienergy (red curve) and corresponding eigenstate (shown by Husimi function) of unitary evolution operator of quantum sawtooth map with strength of static imperfections ϵ:

$$\overline{\psi} = e^{-iT\hat{n}^2/4} e^{ik(\hat{\theta}-\pi)^2/2} e^{-iT\hat{n}^2/4} \psi = e^{-iE}\psi$$

Here $\epsilon = 0,\ 4\times 10^{-4},\ 10^{-3}$ (right top, left/right bottom); and $K = kT = \sqrt{2}, T = 2\pi/N,\ \ N = 2^{n_q}, J = 0, n_q = 9$. Mixing of levels takes place at critical interaction strength:

$$\epsilon_\chi \sim 1/\sqrt{N} \sim 2^{-n_q/2}$$

Random matrix theory for fidelity decay

Fidelity with average initial state: $f(t) = \left| \frac{1}{N} \mathtt{tr} \left(U^{-t} \left(U\, e^{i\delta H_{\rm eff}} \right)^t \right) \right|^2$

Regime $(1-f) \ll 1$: $f(t) \approx 1 - \frac{t}{t_c} - \frac{2}{t_c} \sum_{\tau=1}^{t-1} (t-\tau)\, C(\tau)$

with: $\frac{1}{t_c} = \frac{1}{N} \mathtt{tr} \left({\delta H_{\rm eff}}^2 \right)$, $C(\tau) = \frac{t_c}{N} \mathtt{tr} \left(\underbrace{U^{-\tau}\, \delta H_{\rm eff}\, U^{\tau}}_{\delta H_{\rm eff}(\tau)}\, \delta H_{\rm eff} \right)$

$U \in$ COE (CUE) $\Rightarrow$ Scaling law:

$$-\langle \ln f(t) \rangle_U \approx \frac{N}{t_c} \chi \left(\frac{t}{N} \right) , \quad \chi(s) = s + \frac{2}{\beta}\, s^2 - 2 \int_0^s d\tilde{\tau}\, (s-\tilde{\tau})\, b_2(\tilde{\tau}) \, .$$

with the "two-level form factor": $b_2(\tilde{\tau})$.

Scaling analysis for chaotic dynamics

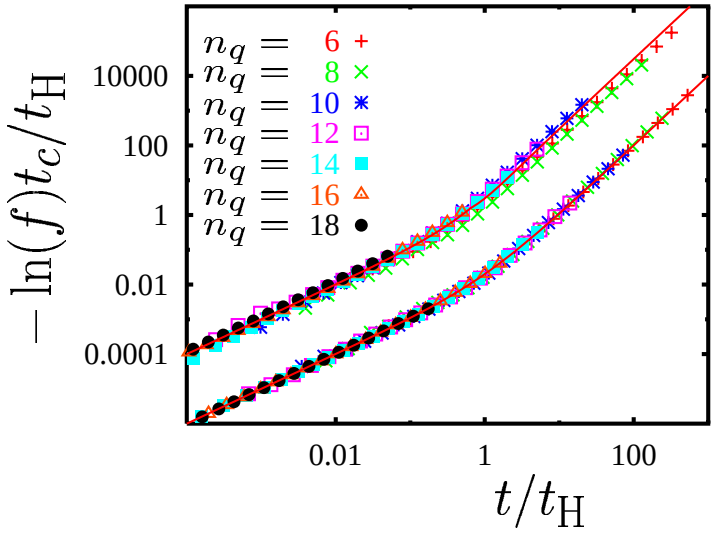

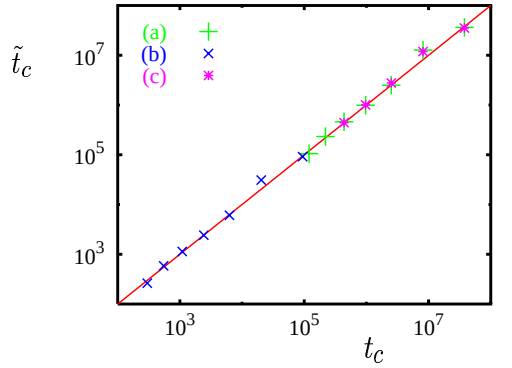

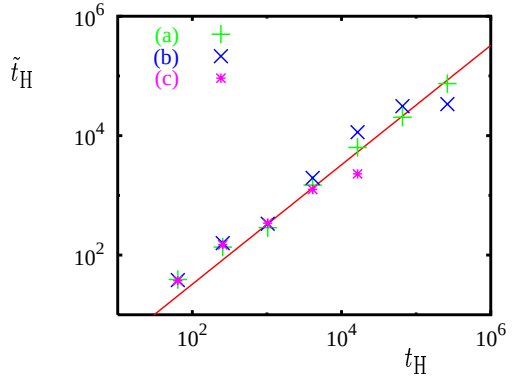

Upper curve: with theoretical values:

$t_{\rm H} = 2^{n_q}$ and $t_c = 1/(\varepsilon^2\, n_q\, n_g^2)$

Lower curve: with fit values $\tilde{t}_c$ and $\tilde{t}_{\rm H}$ from: $-\ln(f(t)) = \dfrac{t}{\tilde{t}_c} + \dfrac{t^2}{\tilde{t}_c \tilde{t}_{\rm H}} \quad (\tilde{t}_{\rm H} \approx t_{\rm H}/3)$

Integrable dynamics

$t = 22783$, Fit: $-\ln(f(t)) = \frac{t}{\tilde{t}_c} + \frac{t^2}{\tilde{t}_c \tilde{t}_{\rm H}}$.

$n_q = 14$

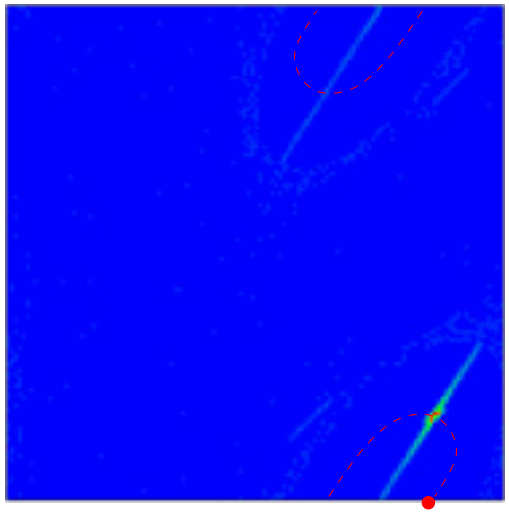

$\varepsilon = 0$

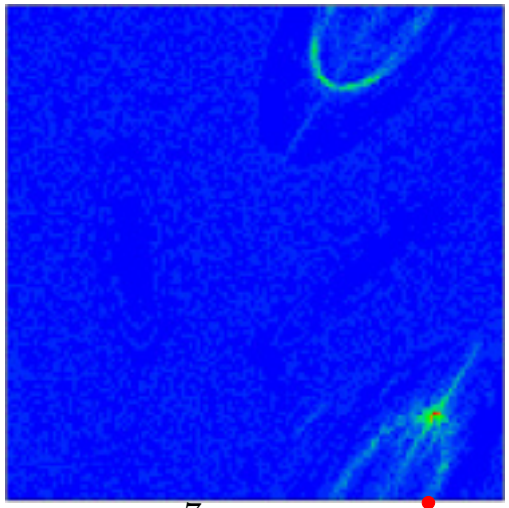

$\varepsilon = 5 \cdot 10^{-7}, \quad f = 0.5$

Position of initial gaussian wave packet

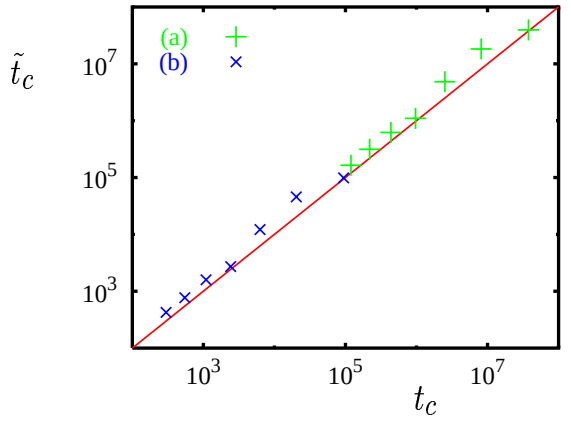

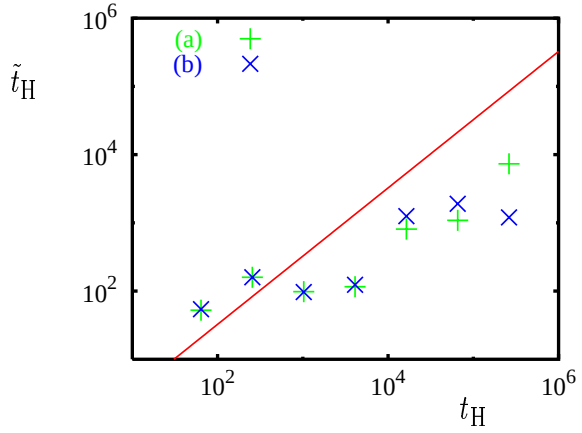

Time scale of reliable quantum computations

Time scale t_f with $f(t_f) = 0.9$:

Theory from RMT-approach:

If $\varepsilon \gg (2^{n_q}\, n_g^2 n_q)^{-1/2}$:

$$t_f \approx 0.1\, t_c \approx 1/(10\varepsilon^2\, n_q\, n_g^2)$$

$$N_g = t_f\, n_g \approx 1/(10\varepsilon^2\, n_q\, n_g)$$

If $\varepsilon \ll (2^{n_q}\, n_g^2 n_q)^{-1/2}$:

$$t_f \approx 0.2\, \sqrt{t_c t_{\rm H}} \approx 2^{n_q/2}/(5\varepsilon\, n_g\, \sqrt{n_q})$$

Random errors: $N_g \approx 5/\varepsilon^2$

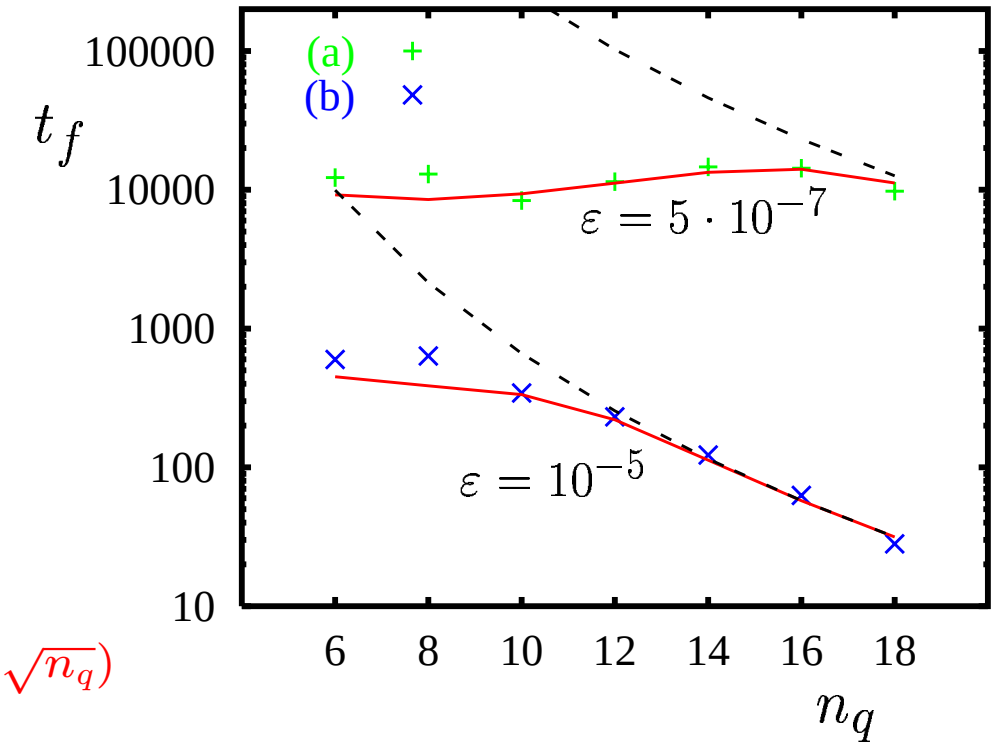

Pauli Random Error Correction (PAREC)

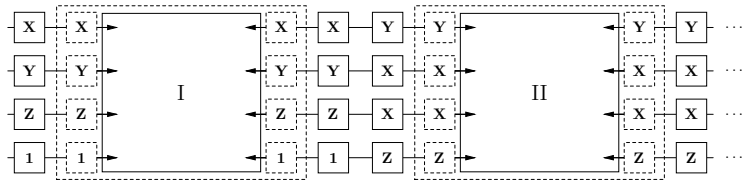

The basic idea of the PAREC-method: The two boxes (full lines) represent two sequences of universal quantum gates for $n_q = 4$ qubits. Two random sequences of Pauli operators $(\hat{X}_1, \hat{Y}_2, \hat{Z}_3, \mathbf{1}_4)$ and $(\hat{Y}_1, \hat{X}_2, \hat{X}_3, \hat{Z}_4)$ are also indicated. The unitary Pauli operators outside the dashed boxes (full lines) are applied to the qubits whereas the ones inside the dashed boxes (dashed lines) are taken into account by appropriate permutations of the elementary quantum gates. Due to the identities $\hat{X}^2 = \hat{Y}^2 = \hat{Z}^2 = \mathbf{1}$ the inserted random sequences of Pauli operators change the computational basis but leave the ideal quantum algorithm unchanged.

The PAREC method eliminates coherent errors produced by static imperfections and increases significantly the maximum time over which realistic quantum computations can be performed reliably. Furthermore, it does not require redundancy using all qubits for logical purposes.

Pauli Random Error Correction (PAREC)

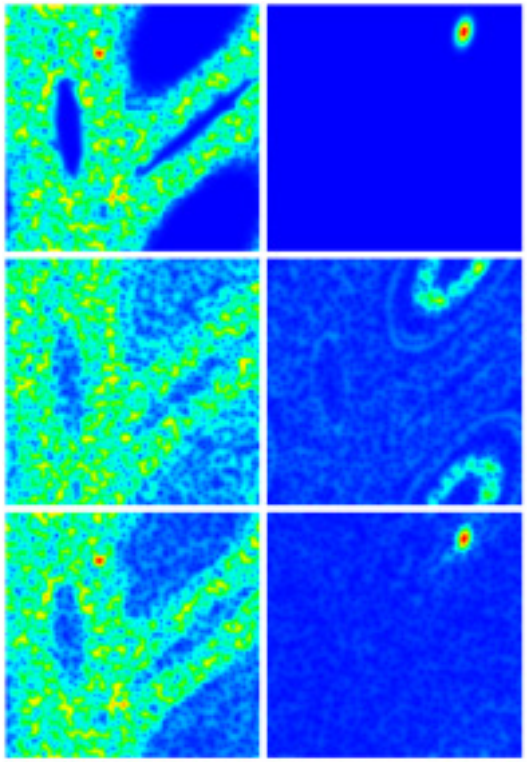

Quantum Poincaré sections with Husimi-functions in tent map at $t = 3000$ in scaled momentum and position variables $\tilde{y} = p \in [0, 2\pi]$ and $\tilde{x} = x \in [0, 2\pi]$: The parameters are $K = 1.7$ and $n_q = 10$. The initially prepared coherent states are centered around $(\pi/4, 0)$ (left panel) and $(5.35, 0)$ (right panel). First row: ideal dynamics; second row: static imperfections with $\epsilon = 5 \times 10^{-6}$; third row: PAREC-method applied after each sequence of $n_{\rm gef} = 20$ universal quantum gates of Ref. [17]. The probability density is coded in colors (red/maximum, blue/zero).

Pauli Random Error Correction (PAREC)

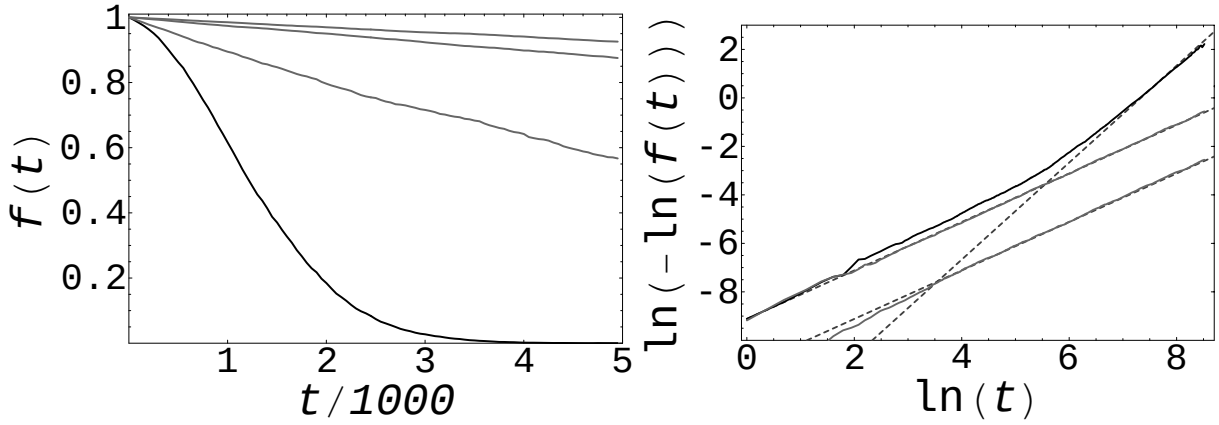

Dependence of the fidelity $f(t)$ on the number of iterations: Parameters as in the left panel of previous Fig.; left: static imperfections without error correction, PAREC after each map iteration, after each $n_{\rm gef} = 50$, and after each $n_{\rm gef} = 20$ quantum gates (from bottom up); right: static imperfections without error correction, with PAREC after each map iteration and after each sequence of $n_{\rm gef} = 20$ quantum gates (full curves), best fits for linear- and quadratic-in-time decays (dashed curves).

Quantum computation of the Anderson transition in presence of imperfections,
Phys.Rev. A **69**, 014302 (2004)

Quantum computation of the Anderson transition in presence of imperfections

The stationary Schrödinger equation for the Anderson model: a particle on a d-dimensional lattice in a random potential: $\sum_{\vec{m}} V_{\vec{m}}\psi_{\vec{m}+\vec{n}} + E_{\vec{n}}\psi_{\vec{n}} = E\psi_{\vec{n}}$, In $d \geq 3$ dimensions the wave functions are exponentially localized for sufficiently large (compared to $V_{\vec{m}}$) typical value of $E_{\mathbf{n}}$ and delocalized for small typical value of $E_{\mathbf{n}}$ (P.W. Anderson (1958)).
Our model: 1-dim. kicked rotator with frequency modulation.
Anderson localization $\longrightarrow$ dynamical localization of quantum chaos in the kicked rotator model (S. Fishman et al. (1982)).
3 dimensions $\longrightarrow$ 1 dimension plus frequency modulation with 2 incomensurate frequencies (D.L.S (1983)).

Our Hamiltonian H: $H_0(n) + k(1 + \epsilon\cos(\Omega_1 t)\cos(\Omega_2 t))\cos\theta\sum_m \delta(t-m)$,
The time evolution: $\bar{\psi} = U_T U_k \psi, \qquad U_T = \exp\{-iH_0(n)\}$
$U_k = \exp\{-ik(1 + 0.75\cos(\Omega_1 t)\cos(\Omega_2 t))\cos\theta\}$.

A. A. Pomeransky and D. L. Shepelyansky

The quantum algorithm

The quantum states $n = 0, ..., N-1$ are represented by one quantum register with n_q qubits so that $N = 2^{n_q}$. The initial state with all probability at $n_0 = 0$ corresponds to the state $|00...0\rangle$ (momentum n changes on a circle with N levels). The random phase multiplication $U_T = \exp(-iH_0(n))$ in the momentum basis is performed as a random sequence of one-qubit phase shifts and controlled-NOT gates. Then the kick operator $U_k = \exp(-ik(t)\cos\theta)$ is performed as follows. First, one applies the QFT to change the representation. Then θ can be written in the binary representation as $\theta/2\pi = 0.a_1a_2..a_{n_q}$ with $a_i = 0$ or 1. It's convenient to use the notation $\theta = \pi a_1 + \bar{\theta}$ to single out the most significant qubit. Then due to the relation $\cos\theta = (-1)^{a_1}\cos\bar{\theta} = \sigma_1^z \cos\bar{\theta}$ the kick operator takes the form $U_k = e^{-ik(t)\cos\theta} = e^{-i\sigma_1^z k(t)\cos\bar{\theta}}$. This operator can be approximated to an arbitrary precision by a sequence of one-qubit gates applied to the first qubit and the diagonal operators $S^m = e^{ima_1\bar{\theta}}$. We used the following sequence: $R_\gamma(\bar{\theta}) = HS^1H\ e^{-i\frac{\gamma}{4}\sigma_1^z}\ HS^{-2}H\ e^{-i\frac{\gamma}{2}\sigma_1^z}\ HS^2H\ e^{-i\frac{\gamma}{4}\sigma_1^z}\ HS^{-1}H = e^{-i\sigma_1^z\gamma\cos(\bar{\theta})} + O(\gamma^3)$, where $H = (\sigma_1^z + \sigma_1^x)/\sqrt{2}$ is the Hadamard gate. Thus the kick operator is given by $U_k = R_\gamma(\bar{\theta})^l + O(l\gamma^3)$, where the number of steps $l = k/\gamma$ and we used in our numerical simulations the small parameter $\gamma = k/l \approx 0.2$ that gives $l \approx 5 - 10$ for $k \sim 1 - 2$. The number of gates is $\sim k$, so the algorithm is more efficient for moderate k. Then one goes back to the momentum representation by the QFT. One complete iteration of the algorithm requires n_g elementary gates where $n_g = 2[k/\gamma](n_q + 2) + n_q^2 + 12n_q + 9$ with the square brackets denoting the integer part.

Static imperfections in QA for Anderson transition

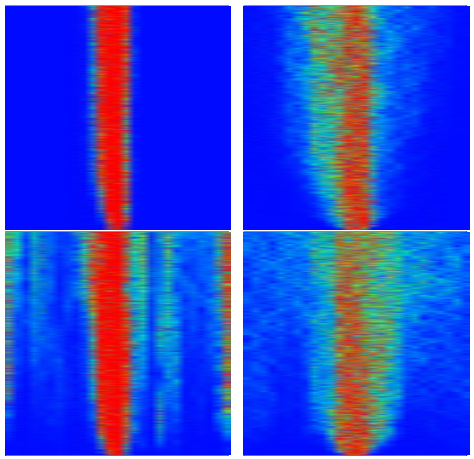

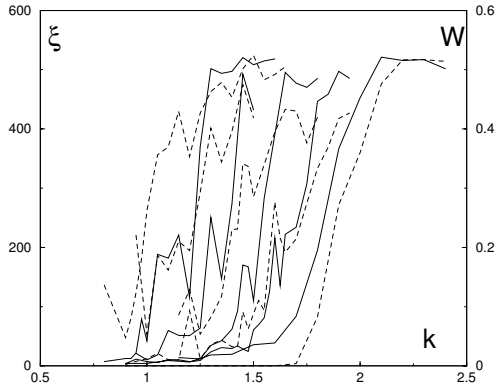

The time evolution of the probability distribution $|\psi_n|^2$ in the localized (left column, $k = 1.2$) and delocalized (right column, $k = 2.4$) phases for $n_q = 7$ qubits ($N = 2^{n_q}$), with $0 \leq t \leq 400$ (vertical axis) and $-N/2 < n \leq N/2$ (horizontal axis); $k_c = 1.8$. The strength of static imperfections is $\epsilon = \mu = 0$ for top row and $\epsilon = \mu = 10^{-4}$ for bottom row.

Dependence of the IPR ξ and the excitation probability: $W = \sum_{n=(N/4,3N/4)} |\psi_n|^2$ (full and dashed curves for left and right scales respectively) on the kick strength k for $n_q = 10$ and $t \geq 10^5$, $\epsilon = 0$; 10^{-5}; $2{\times}10^{-5}$; $4{\times}10^{-5}$; $8{\times}10^{-5}$ (curves from right to left); $\mu = 0$.

Critical point shift

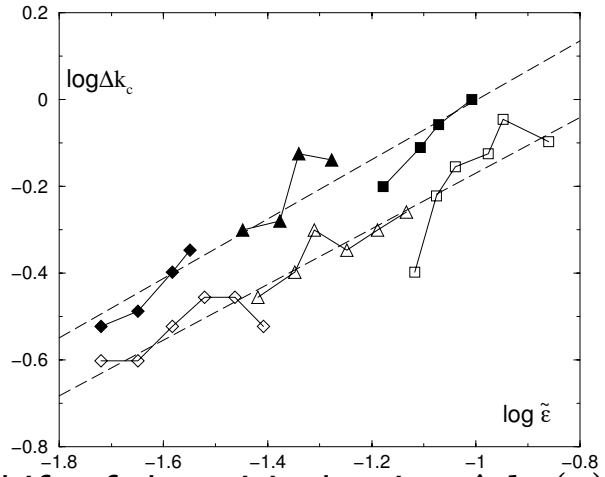

Dependence of the shift of the critical point $\Delta k_c(\epsilon) = k_c - k_c(\epsilon)$ on rescaled imperfection strength $\tilde{\epsilon} = \epsilon n_g \sqrt{n_q}$ for $\epsilon = 2 \times 10^{-5}$ (diamonds), 4×10^{-5} (triangles) and 8×10^{-5} (squares); open/full symbols are for $\mu = 0$, $8 \leq n_q \leq 13$ and $\mu = \epsilon$, $8 \leq n_q \leq 11$ respectively; $k_c = 1.8$. The dashed lines show the scaling relation.

The shift of the critical point $\Delta k_c(\epsilon) = k_c - k_c(\epsilon)$ depends on ϵ, μ and n_q. From the IPR data obtained for various ϵ, μ, n_q we find that the global parameter dependence can be described by the scaling relation $\Delta k_c(\epsilon) = A \tilde{\epsilon}^{\,\alpha}$, $\tilde{\epsilon} = \epsilon n_g \sqrt{n_q}$. The data fit gives $A = 3.0$, $\alpha = 0.64$ for $\mu = 0$ and $A = 4.8$, $\alpha = 0.68$ for $\mu = \epsilon$.

In the vicinity of the critical point the algorithm gives a quadratic speedup in computation of diffusion rate and localization length, comparing to the known classical algorithms.

The complexity of quantum algorithm

The quantum states $n = 0, ..., N-1$ are represented by one quantum register with n_q qubits so that $N = 2^{n_q}$. The initial state with all probability at $n_0 = 0$ corresponds to the state $|00...0\rangle$ (momentum n changes on a circle with N levels). The random phase multiplication $U_T = \exp(-iH_0(n))$ in the momentum basis is performed as a random sequence of one-qubit phase shifts and controlled-NOT gates. Then the kick operator $U_k = \exp(-ik(t)\cos\theta)$ is performed. One complete iteration of the algorithm requires n_g elementary gates where $n_g \approx 10k(n_q+2) + n_q^2$.

However, in the vicinity of critical point in real d-dimensions the number of states grows with time as $n^d \sim t$. Hence, up to time t the classical computation may use only N levels in each direction so that the total number of levels is $N^d \sim t$. Other levels are only very weakly populated on this time scale and therefore they can be eliminated with a good accuracy. Thus, the number of classical operations for t kicks can be estimated as $n_{gcl} \sim tN^d \log^d N \sim t^2 \log^d t$. At the same time the quantum algorithm will need $n_g \sim dn_q^2 t \sim t \log^2 t$ gates assuming d quantum registers with $N^d = 2^{dn_q} \sim t$ states. The coarse-grained characteristics of the probability distribution can be determined from few measurements of most significant qubits, *e.g.* W. Thus, even if each iteration step is efficient, the speedup is only quadratic near the critical point.

Phase diagram for the Grover algorithm with static imperfections,
Eur. Phys. J. D **31**, 131 (2005)

Phase diagram for the Grover algorithm with static imperfections

An unstructured database is presented by $N = 2^{n_q}$ states of quantum register with n_q qubits: $\{|x\rangle\}$, $x = 0, \ldots, N-1$. The searched state $|\tau\rangle$ can be identified by *oracle* function $g(x)$, defined as $g(x) = 1$ if $x = \tau$ and $g(x) = 0$ otherwise. The Grover iteration operator $\hat{G}$ is a product of two operators: $\hat{G} = \hat{D}\hat{O}$. Here the oracle operator $\hat{O} = (-1)^{g(\hat{x})}$ is specific to the searched state $|\tau\rangle$, while the diffusion operator $\hat{D}$ is independent of $|\tau\rangle$: $D_{ii} = -1 + \frac{2}{N}$ and $D_{ij} = \frac{2}{N}$ $(i \neq j)$. For the initial state $|\psi_0\rangle = \sum_{x=0}^{N-1} |x\rangle/\sqrt{N}$, t applications of the Grover operator $\hat{G}$ give:

$$|\psi(t)\rangle = \hat{G}^t|\psi_0\rangle = \sin\left((t+1)\omega_G\right)|\tau\rangle + \cos\left((t+1)\omega_G\right)|\eta\rangle$$

where the Grover frequency $\omega_G = 2\arcsin(\sqrt{1/N})$ and $|\eta\rangle = \sum_{x\neq\tau}^{(0\leq x<N)} |x\rangle/\sqrt{N-1}$. Hence, the ideal algorithm gives a rotation in the 2D plane $(|\tau\rangle, |\eta\rangle)$.

A. A. Pomeransky, O. V. Zhirov and D. L. Shepelyansky

The implementation of the operator D through the elementary gates requires an ancilla qubit. As a result the Hilbert space becomes a sum of two subspaces $\{|x\rangle\}$ and $\{|x+N\rangle\}$, which differ only by a value of (n_q+1)-th qubit. These subspaces are invariant with respect to operators O and D: $O = 1 - 2|\tau\rangle\langle\tau| - 2|\tau+N\rangle\langle\tau+N|$, $D = 1 - 2|\psi_0\rangle\langle\psi_0| - 2|\psi_1\rangle\langle\psi_1|$, where $|\psi_1\rangle = \sum_{x=0}^{N-1}|x+N\rangle/\sqrt{N}$ and $|\psi_{0,1}\rangle$ correspond to up/down ancilla states. Then D can be represented as $D = WRW$ (Grover (1997)), where the transformation $W = W_{nq}\ldots W_k\ldots W_1$ is composed from n_q one-qubit Hadamard gates W_k, and R is the n_q-controlled phase shift defined as $R_{ij} = 0$ if $i \neq j$, $R_{00} = 1$ and $R_{ii} = -1$ if $i \neq 0$ $(i,j = 0,\ldots,N-1)$. In turn, this operator can be represented as $R = W_{nq}\sigma^x_{nq-1}\ldots\sigma^x_1 \wedge_{nq} \sigma^x_{nq-1}\ldots\sigma^x_1 W_{nq}$, where $\wedge_{nq}$ is generalized n_q-qubit Toffolli gate, which inverts the n_q-th qubit if the first n_q-1 qubits are in the state $|1\rangle$. The construction of $\wedge_{nq}$ from 3-qubit Toffolli gates with the help of only one auxillary qubit is described by A.Barenco *et al.* (1995). As a result the Grover operator G is implemented through $n_g = 12n_{tot} - 42$ elementary gates including one-qubit rotations, control-NOT and Toffolli gates. Here $n_{tot} = n_q + 1$ is the total number of qubits.

Oscillations of the Grover search probability

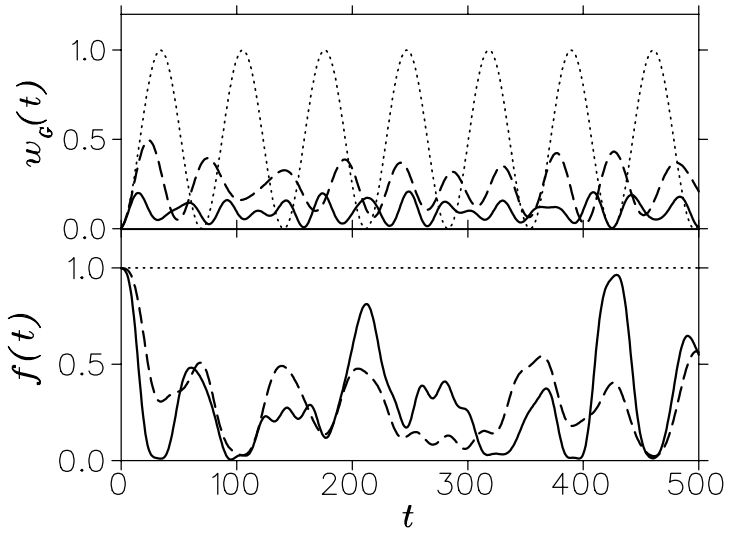

Probability of searched state $w_G(t)$ (top) and fidelity $f(t)$ (bottom) as a function of the iteration step t in the Grover algorithm for $n_{tot} = 12$ qubits. Dotted curves show results for the ideal algorithm ($\varepsilon = 0$), dashed and solid curves correspond to imperfection strength $\varepsilon = 4 \cdot 10^{-4}$ and 10^{-3}, respectively.

A typical example of imperfection effects on the accuracy of the Grover algorithm for a fixed disorder realization of H_S on 3×4 qubit lattice.

Phase diagram for the Grover algorithm with static imperfections,
Eur. Phys. J. D **31**, 131 (2005)

Husimi function in the Grover algorithm

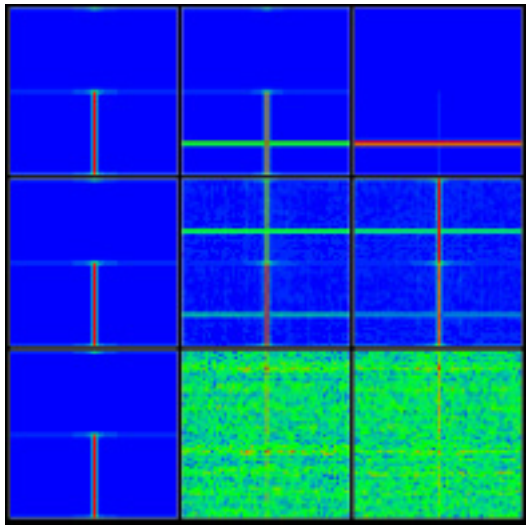

Evolution of the Husimi function in the Grover algorithm at times $t = 0$, 17, and 34 (from left to right), and for $\varepsilon = 0$, 0.001, and 0.008 (from top to bottom). The qubit lattice and disorder realization are the same as in previous Fig. The vertical axis shows the computational basis $x = 0, \ldots, 2N - 1$, while the horizontal axis represents the conjugated momentum basis. Density is proportional to color changing from maximum (red) to zero (blue).

the probability is mainly distributed over four states corresponding to four straight lines in phase space: $|\tau_0\rangle = |\tau\rangle$; $|\tau_1\rangle = |\tau + N\rangle$; $|\eta_0\rangle = |\eta\rangle$; $|\eta_1\rangle = \sum_{x\neq\tau}^{(0\leq x<N)} |x + N\rangle/\sqrt{N-1}$

A. A. Pomeransky, O. V. Zhirov and D. L. Shepelyansky

Phase diagram for spectral density

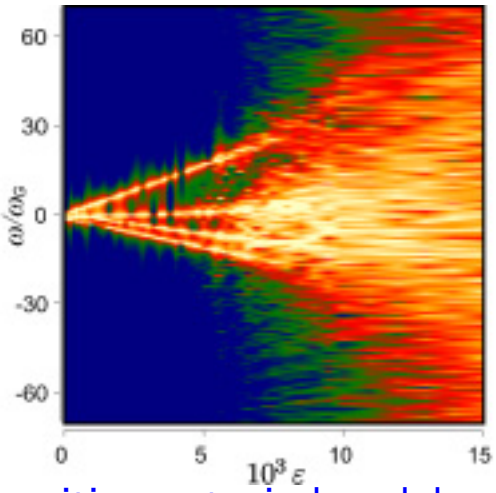

Phase diagram for the spectral density $S(\omega)$ as a function of imperfection strength ε, $n_{tot} = 12$, same disorder realization as in previous Fig. Color is proportional to density $S(\omega)$ (yellow for maximum and blue for zero).

The transition rate induced by imperfections after one Grover iteration is given by the Fermi golden rule: $\Gamma \sim \varepsilon^2 n_g^2 n_{tot}$, where n_{tot} appears due to random contribution of qubit couplings ε while n_g^2 factor takes into account coherent accumulation of perturbation on n_g gates used in one iteration. In the Grover algorithm the four states are separated from all other states by energy gap $\Delta E \sim 1$ (sign change introduced by operators O and D). Thus these four states become mixed with all others for $\varepsilon > \varepsilon_c \approx 1.7/(n_g\sqrt{n_{tot}})$, when $\Gamma > \Delta E$.

Averaging over disorder

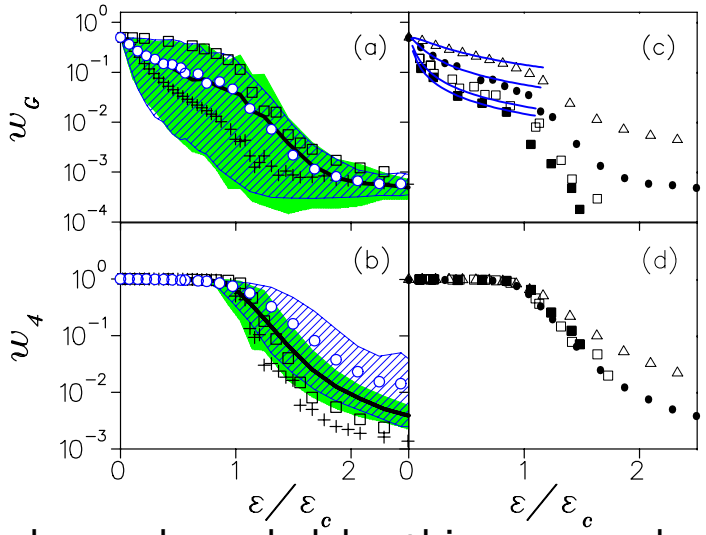

Dependence of probabilities w_G (a,c) and w_4 (b,d) on rescaled imperfection strength $\varepsilon/\varepsilon_c$. For panels (a,b) $n_{tot} = 12$, squares and pluses show data for two typical disorder realizations, green/grey area shows the region of probability variation for various disorder realizations (see text), full thick curves give average dependence $\bar{w}_G$, $\bar{w}_4$.

Dashed area bounded by thin curves show the region of probability variation in the single-kick model, open circles give the average data in this model with rescaling factor $R = 0.56$. Panels (c,d) show $\bar{w}_G$, $\bar{w}_4$ for $n_{tot} = 9$ (triangles), 12 (full circles), 15 (open squares) and 16 (full squares). In panel (c) full curves are given by theory for same n_{tot} values from top to bottom, $R = 0.56$.

Theoretical estimates for the Grover algorithm

In the regime where the dynamics of Grover algorithm is dominated by four states subspace the single-kick model can be treated analytically. The matrix elements of the effective Hamiltonian in this space are

$$H_{eff} = \begin{pmatrix} A+a & 0 & -i\omega_G & 0 \\ 0 & A-a & 0 & -i\omega_G \\ i\omega_G & 0 & B & b \\ 0 & i\omega_G & b & B \end{pmatrix}, \tag{1}$$

where $A = -Rn_g \sum_{i=1}^{n_q} a_i \langle\tau|\sigma_i^{(z)}|\tau\rangle$, $B = Rn_g \sum_{i<j}^{n_q} b_{i,j} - b$, $a = -Rn_g a_{nq+1}$ and $b = Rn_g(b_{nq+1,nq+2-Lx} + b_{nq+1,Lx} + b_{nq,nq+1} + b_{nq+1-Lx,nq+1})$ and qubits are arranged on $L_x \times L_y$ lattice, and numerated as $i = x + L_x(y-1)$, with $x = 1, \ldots, L_x$, $y = 1, \ldots, L_y$. In the limit of large n_q the terms a, b are small compared to A, B by a factor $1/\sqrt{n_q}$ and H_{eff} is reduced to 2×2 matrix, which gives $w_G = 2\omega_G^2/[(A-B)^2 + 4\omega_G^2]$.

For large n_q the difference $A - B$ has a Gaussian distribution with width $\sigma = Rn_g\sqrt{n_q/3}\sqrt{\alpha^2+2\beta^2} = \varepsilon Rn_g\sqrt{n_q}$. The convolution of w_G with this distribution gives

$$\bar{w}_G = \sqrt{\pi/2}(1 - erf(\sqrt{2}\omega_G/\sigma))\exp(2\omega_G^2/\sigma^2)\,\omega_G/\sigma \qquad (2)$$

This formula gives a good description of numerical data in Fig. c that confirms the validity of single-kick model. For $\sigma \gg \omega_G$ and a typical disorder realization with $(A-B) \sim \sigma$ the actual frequency of Grover oscillations is strongly renormalized: $\omega \approx (A-B) \sim \sigma \gg \omega_G$, and in agreement with previous Fig. $\omega \sim \varepsilon/\varepsilon_c$. In this typical case $w_G \sim \omega_G^2/\sigma^2 \ll 1$ (almost total probability is in the states $|\eta_0\rangle$,$|\eta_1\rangle$). Hence, the total number of quantum operations N_{op}, required for detection of searched state $|\tau\rangle$, can be estimated as $N_{op} \sim N_M/\omega \sim \sigma/\omega_G^2 \sim \varepsilon N/\varepsilon_c$, where $N_M \sim 1/w_G \sim \sigma^2/\omega_G^2$ is a number of measurements required for detection of searched state. Thus, in presence of strong static imperfections the parametric efficiency gain of the Grover algorithm compared to classical one is of the order $\varepsilon_c/\varepsilon$. For $\varepsilon \sim \omega_G$ the efficiency is comparable with that of the ideal Grover algorithm while for $\varepsilon \sim \varepsilon_c$ there is no gain compared to the classical case.